J. Fluid Mech. (1979), *vol.* 94, *part* 3, *pp.* 595–607
Printed in Great Britain

A simple model of the mutual interaction of parallel flow and cellular motion in a shear layer applied to the finite amplitude instability of plane Couette flow

By J. STEPPELER
Deutscher Wetterdienst, Offenbach, BRD

(Received 12 October 1977 and in revised form 25 October 1978)

The disturbing motion of plane Couette and Poiseuille flow is described using three parameters: two amplitudes corresponding to the disturbance of the parallel flow and the cellular motion, respectively, and the angle ϕ_0 which defines the orientation of the vortex blobs with respect to the parallel flow. Equations of motion for these parameters are obtained using a Ritz–Galerkin method. For Reynolds numbers above a critical value sufficiently big disturbances will grow until a steady finite amplitude state is achieved. The energy of the disturbance remains finite, in spite of the highly truncated field representation using only three parameters. This is possible because of the nonlinear dependence of the field functions on ϕ_0. The critical values of Reynolds number, above which finite amplitude states exist, are computed for the plane Couette flow and the Poiseuille channel flow.

1. Introduction

According to a number of investigations the plane Couette flow is stable with respect to infinitesimal disturbances (Grohne 1954; Gallagher & Mercer 1964; Davey 1973). It is generally supposed that the plane Couette flow is unstable with respect to sufficiently large disturbances which must be computed by taking into account nonlinear effects.

The approach to approximate finite amplitude solutions of the Navier–Stokes equations was given by Stuart (1958, 1960) and Watson (1960). Explicit calculations have been done concerning the instability of the plane channel flow (Reynolds & Potter 1967; Pekeris & Shkoller 1969*a*, *b*). As expected, these theories provided growing finite amplitude solutions for Reynolds numbers in the stable region of the Orr–Sommerfeld theory.

For some of these theories the solutions grow without bound if the initial disturbances are big enough. This applies even to theories which do not have an explicit small amplitude limitation (Pekeris & Shkoller 1969*a*, 1971). This unphysical behaviour seems to be caused by the coarse truncation of the respective methods. In fact, with present-day computers, the number of constants used to describe the field for a fixed time always requires some compromises. In reality the nonlinear effects will place a limitation on the amplitude of the disturbance. As pointed out by Zahn *et al.* (1974), a good resolution of the cross-stream structure of the solution will lead to limited amplitude solutions in the fluid model. Some of the cross-stream resolution

0022-1120/79/4298-7480 $02.00

can be saved by using a numerically highly accurate discretization. This was done by Herbert (1976) using a method inspired by Orszag (1971).

However, in view of the arguments given by Zahn *et al.* (1974), one cannot use too few gridpoints in the cross-stream co-ordinate if one wants to obtain disturbed states of limited amplitude. In the model of Pekeris & Shkoller (1969*b*) the unboundedness of the disturbance amplitudes seems to be caused by the drastically truncated eigenfunction representation. In contrast to this, the resolution in the downstream direction seems to have less influence on the physical behaviour of the solution. Zahn *et al.* (1974) obtained steady finite amplitudes solutions using a drastically truncated Fourier representation in the downstream direction.

So far, all computations without explicit finite amplitude limitation and resulting in quasi-stationary finite amplitude states were done with respect to the Poiseuille flow. Much less is known concerning the nonlinear theory of plane Couette flow. Coffee (1977) investigated the problem by perturbation theory. Because of the explicit finite amplitude limitation of this method, the solution was quite inaccurate for small Reynolds numbers. Rather as in the Poiseuille flow case, the perturbation theory results in a perturbed quasi-stationary solution for every Reynolds number. In contrast to this, theories without small amplitude limitation should result in perturbed solutions only for sufficiently large Reynolds number.

The present paper investigates a very simple model of the secondary motion of plane Couette and Poiseuille flow, using a Ritz–Galerkin method with only three parameters to specify a fluid state at a fixed time. Such highly simplified models of fluid motion are known for the Bénard convection flow. These models were investigated by Lorenz (1963) and Ogura & Yagihashi (1969) for the free-slip boundary case and by Steppeler (1978) for the case where all velocity components vanish at the boundary. For the Bénard flow, it is relatively easy to construct simplified models of the fluid motion, because a linear space of test functions turns out to be sufficient. However, for the Poiseuille flow the work of Zahn *et al.* (1974) indicates that, without using a great number of dynamic parameters, no quasi-stationary finite amplitude states will be obtained with a linear dependence of the test functions on the parameters which describe a state.

Existing models of the secondary motion of the plane Poiseuille flow have, until now, used a linear dependence of the field functions on the parameters $\lambda_1, \ldots, \lambda_n$ which describe the physical state at a fixed time:

$$\psi(X, Y, t) = \sum_{\nu} \lambda_\nu(t)\, \phi_\nu(X, Y).$$

To represent sufficiently many fluid states, one must use models with a considerable number of constants $\lambda_1, \ldots, \lambda_n$.

In the present paper we will use two amplitude parameters and an angle ϕ_0 to specify fluid states for the plane Couette and the Poiseuille flow. The dependence of the field on ϕ_0 will be nonlinear. Therefore we obtain a great number of linearly independent states for different values of ϕ_0.

If a certain profile of the parallel flow is given, this family of states includes those which are damped and others which are amplified when treated by the linearized equations. The nonlinear interactions cause a transition to linearly stable states for sufficiently large amplitudes. Therefore the three-parameter model is able to have quasi-stationary finite amplitude states.

The particular model, described in § 3, was motivated by physical considerations. The real and imaginary parts of the Orr–Sommerfeld eigenfunction represent two systems of vortices which overlap. Similar to the vortex lines in an ideal fluid, the centres of these vortices can be expected to rotate around each other for finite amplitudes. The model was chosen to represent this effect in a rough manner.

The secondary flow will be assumed to be a system of vortex blobs, which are regions of finite extent of the fluid with a cellular motion. Similar flow fields can be seen when observing a turbulent shear flow with a moving camera. Parameters which describe the relative position of the blobs were introduced as dynamic parameters.

2. Basic equations and approximations

We start from the Navier–Stokes equations for two-dimensional motion of an incompressible fluid

$$\left.\begin{aligned} U_t + UU_x + VU_y - \frac{1}{Re}\Delta U &= -P_x, \\ V_t + UV_x + VV_y - \frac{1}{Re}\Delta V &= -P_y, \\ U_x + V_y &= 0; \end{aligned}\right\} \tag{1}$$

and the boundary conditions for the plane Couette flow

$$V = 0, \quad U = \pm 1 \quad \text{for} \quad Y = \pm 1; \tag{2}$$

and for the plane Poiseuille flow

$$V = U = 0 \quad \text{for} \quad Y = \pm 1,$$

$$\int_{X_1}^{X_2} P_x \, dx \to 2\frac{X_2 - X_1}{Re} \quad \text{for} \quad X_2 - X_1 \to \infty.$$

We introduce the stream function ψ and vorticity ξ by

$$U = \psi_y, \quad V = -\psi_x, \quad \xi = U_y - V_x = \Delta\psi, \tag{3}$$

and obtain by eliminating P from (1)

$$\psi_t + U\,\Delta\psi_x + V\,\Delta\psi_y - \frac{1}{Re}\Delta\Delta\psi = 0. \tag{4}$$

Defining the operation $\overline{}^x$ by

$$\overline{\alpha}^x = \frac{1}{L}\int_x^{x+L} dx'\,\alpha(x')$$

and applying this operation to the first of the equations (1). When assuming all fields to be periodic in the X direction with periodicity length L we obtain for the Couette flow

$$\overline{U}_t^x + \overline{VU_y}^x - \frac{1}{Re}\overline{U}_{yy}^x = 0; \tag{5}$$

and for the Poiseuille flow

$$\overline{U}_t^x + \overline{VU_y}^x - \frac{1}{Re}\overline{U}_{yy}^x = -\frac{2}{Re}.$$

The undisturbed solution of (1) and (2) is for the Couette flow

$$U = Y, \quad V = 0, \tag{6}$$

and for the Poiseuille flow

$$U = Y^2 - 1, \quad V = 0.$$

We assume a perturbation motion which is specified by a set of parameters $\lambda_1, \ldots, \lambda_n$.

For the Couette flow we use

$$\psi = \tfrac{1}{2}Y^2 + \phi(X, Y, \lambda_1, \ldots, \lambda_n), \tag{7}$$

and for the Poiseuille flow

$$\psi = \tfrac{1}{3}Y^3 - Y + \phi(X, Y, \lambda_1, \ldots, \lambda_n).$$

Every choice of a function $\phi(X, Y, \lambda_1, \ldots, \lambda_n)$ will result in a nonlinear model. To obtain the time development of $\lambda_1, \ldots, \lambda_n$, we will use a Ritz method. The least square functional Q will be minimized in the limit of small time intervals Δt. As we consider Q in the limit $\Delta t \to 0$, it will be possible to neglect terms $O(\Delta t^2)$ of the functional. The method outlined in the following is equivalent to the Galerkin method proposed by Vichenevetsky (1969).

We will use the least square functional

$$Q = \int_t^{t+\Delta t} dt' \int dx\, dy \left(\Delta\psi_t + \psi_y \Delta\psi_x - \psi_x \Delta\psi_y - \frac{1}{Re}\Delta\Delta\psi\right)^2 \tag{8}$$

and apply the test functions given by (7). In equation (7) $\lambda_1, \ldots, \lambda_n$ are now functions from t'. We will consider $\lambda_\nu(t)$ as given and will minimize (8) to obtain $\lambda_\nu(t+\Delta t)$. The use of the least square functional as a variational principle poses some problems (Finlayson 1972; Eason 1976).

Consider (8) as a functional of $\lambda(t')$ and take the Euler equations of Q. These will turn out to be of second order in t'. $\lambda(t)$ is given as initial value but this is not enough to determine the solution of a second-order equation uniquely.

It can be shown that these problems disappear when the variation is taken sufficiently unrestricted. The Euler equation is equivalent to a variation where $\lambda_\nu(t')$ is kept fixed for $t' = t$ and $t' = t + \Delta t$. When keeping $\lambda(t')$ fixed only for $t' = t$, the variation is equivalent to the Euler equation and an additional initial condition (Eason 1976). This is sufficient to determine $\lambda(t')$ uniquely.

Instead of using the least square functional for some finite time interval Δt, we will minimize Q in the limit of small Δt. For small Δt we put

$$\lambda(t') = \lambda(t) + (t' - t).\dot{\lambda}(t) \quad \text{for} \quad t' \in [t, t+\Delta t] \tag{9}$$

and vary with respect to $\dot{\lambda}_\nu(t)$. After variation we will make the transition $\Delta t \to 0$. This means that we must retain only terms $O(\Delta t)$ and can disregard terms $O(\Delta t^2)$.

From (7) and (8) we obtain for the functional Q,

$$Q = \int_t^{t+\Delta t} dt' \int dx\, dy\, F(X, Y, \lambda_1(t'), \ldots, \lambda_n(t')) \tag{10}$$

with

$$F(X, Y, \lambda_1, \ldots, \lambda_n) = \Big(\Delta\psi_t(X, Y, \lambda_1, \ldots, \lambda_n) + \psi_y(X, Y, \lambda_1, \ldots, \lambda_n)\Delta\psi_x(X, Y, \lambda_1, \ldots, \lambda_n) - \psi_x(X, Y, \lambda_1, \ldots, \lambda_n)\Delta\psi_y(X, Y, \lambda_1, \ldots, \lambda_n) - \frac{1}{Re}\Delta\Delta\psi(X, Y, \lambda_1, \ldots, \lambda_n)\Big)^2; \tag{11}$$

Q will be varied according to

$$\delta Q = \int_t^{t+\Delta t} dt' \int dx\, dy \frac{\partial F}{\partial \lambda_\nu} \delta\lambda_\nu + \frac{\partial F}{\partial \dot{\lambda}_\nu} \delta\dot{\lambda}_\nu. \tag{12}$$

Using (9) we obtain

$$\delta Q = \int dx\, dy \sum_\nu \left(\frac{\partial F}{\dot{\lambda}_\nu} \Delta t + \int_t^{t+\Delta t} dt' \frac{\partial F}{\partial \lambda_\nu} (t'-t) \right) \delta\dot{\lambda}_\nu(t). \tag{13}$$

The second term in (13) is $O(\Delta t^2)$. So we can write

$$\delta Q = \left(\Delta t \int dx\, dy \frac{\partial F}{\partial \dot{\lambda}_\nu} + O(\Delta t^2) \right) \delta\dot{\lambda}_\nu(t). \tag{14}$$

To obtain an equation for λ_ν, divide (14) by Δt, put the coefficients of $\partial\lambda_\nu$ to zero separately and let $\Delta t \to 0$. When using the special form of F, equation (11), we obtain:

$$O = \int dx\, dy \frac{\partial \Delta\psi}{\partial \lambda_\mu} \left(\sum_\nu \frac{\partial \Delta\psi}{\partial \lambda_\nu} \dot{\lambda}_\nu + \psi_y \Delta\psi_x - \psi_x \Delta\psi_y - \frac{1}{Re} \Delta\Delta\psi \right). \tag{15}$$

The arguments $X, Y, \lambda_1(t'), \ldots, \lambda_n(t')$ of ψ were dropped in (15). After performing the X–Y integration $\dot{\lambda}_\nu$ occurs in a linear expression. After solving for $\lambda_1, \ldots, \lambda_n$ (15) is an initial value problem for the λ_ν.

Now suppose that ψ in (7) has the form

$$\psi = h(Y) + \phi_1(Y, \lambda_1, \ldots, \lambda_r) + \phi_2(X, Y, \lambda_{r+1}, \ldots, \lambda_n), \tag{16}$$

where ϕ_1 is the stream function belonging to a parallel flow in the X direction. Now (15) will be used to obtain equations only for $\lambda_{r+1}, \ldots, \lambda_n$. The equations for $\lambda_1, \ldots, \lambda_r$ are obtained by the variation of the least square functional belonging to (5). As a result of variation we obtain

$$O = \int dy \frac{\partial \overline{\psi}_y^x}{\partial \lambda_\mu} \left(\left(\sum_\nu \frac{\partial \overline{\psi}_y^x}{\partial \lambda_\nu} \dot{\lambda}_\nu \right) - \overline{\frac{\partial \psi}{\partial X} \frac{\partial^2 \psi}{\partial Y^2}}^x - \frac{1}{Re} \frac{\partial^3 \psi}{\partial Y^3} + \frac{\epsilon}{Re} \right). \tag{17}$$

with $\epsilon = 2$ for the plane Poiseuille flow and $\epsilon = 0$ for the plane Couette flow. In § 3 this formalism will be applied to a very simple model of the disturbed Couette flow.

3. Specification of a simple model

The cellular motion in our model will be represented by three overlapping rotationally symmetric vortex blobs. These can be expected to rotate around each other. The test functions in (7) are specified in the following manner:

$$\psi = h(Y) + \lambda \int_0^y dy' f(Y') + A\overline{\psi}_2(X, Y, \phi_0) \tag{18}$$

with

$$\psi_2(X, Y, \phi_0) = \sum_\nu g\left(\left| \begin{pmatrix} X+\nu\delta \\ Y \end{pmatrix} - r_0 \begin{pmatrix} \cos\phi_0 \\ \sin\phi_0 \end{pmatrix} \right| \frac{2}{a} \right) + g\left(\left| \begin{pmatrix} X+\nu\delta \\ Y \end{pmatrix} \right| \eta \frac{2}{a} \right) + g\left(\left| \begin{pmatrix} X+\nu\delta \\ Y \end{pmatrix} + r_0 \begin{pmatrix} \epsilon' \cos\phi_0 \\ \sin\phi_0 \end{pmatrix} \right| \frac{2}{a} \right);$$

$h(Y) = \frac{1}{2}Y^2$ for the plane Couette flow and $h(Y) = \frac{1}{3}Y^3 - Y$ for the Poiseuille flow. δ is the repetition frequency of the cellular motion, a is the radius of the outer vortex

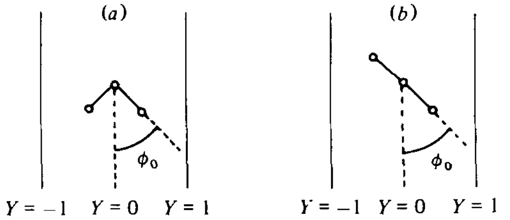

FIGURE 1. The relative positions of the vortex blobs. (a) Poiseuille flow. (b) Plane Couette flow.

blobs, η is the relation of the radius of the outer blobs to that of the centre blob. The parameter ϵ' is 1 for the plane Couette flow and -1 for the Poiseuille flow. The relative positions of the three vortex blobs for the two cases are shown in figure 1.

For the function $g(r)$ we use a piecewise seventh degree polynomial such that g becomes three times differentiable:

$$g(r) = a_0 + a_1(r-1) + a_3(r-1)^3 + a_5(r-1)^5 + (r-1)^7 \tag{19}$$

for $r \in [0, 2]$ and $g(r) = 0$ otherwise with

$$a_5 = -\tfrac{21}{5}, \quad a_3 = 7, \quad a_1 = -7, \quad a_0 = \tfrac{16}{5}.$$

$f(y)$ is defined as a piecewise second-order polynomial which is once differentiable. For the plane Couette flow we will use

$$f(Y) = \begin{Bmatrix} -\dfrac{y}{\alpha} + \gamma_1 y(y-\alpha) & \text{for} \quad y \in [0, \alpha], \\ -\dfrac{\frac{1}{2}-y}{\frac{1}{2}-\alpha} + \gamma_2 (y-\alpha)(y-\frac{1}{2}) & \text{for} \quad y \in [\alpha, \frac{1}{2}], \\ 0 & \text{for} \quad y \in [\frac{1}{2}, 1], \end{Bmatrix} \tag{20}$$

$$f(-Y) = -f(Y);$$

with α being a fixed parameter and

$$\gamma_1 = \frac{\frac{1}{2}+\alpha}{\alpha^2(\frac{1}{2}-\alpha)}, \quad \gamma_2 = \frac{-1}{(\frac{1}{2}-\alpha)^2}.$$

For the plane Poiseuille flow we will use

$$f(Y) = \begin{Bmatrix} 1 + (y^2 - \alpha^2)\gamma_3 & \text{for} \quad y \in [0, \alpha], \\ \dfrac{(1-y)}{1-\alpha} & \text{for} \quad y[\alpha, 1], \end{Bmatrix} \tag{21}$$

$$f(-Y) = f(Y);$$

with α being a fixed parameter and $\gamma_3 = \dfrac{-1}{2\alpha(1-\alpha)}$.

The parameters λ, A, ϕ_0 specify a fluid state and will be used as dynamical variables. The parameters r_0, a, δ are kept fixed. These parameters must be chosen so that no choice of ϕ_0 forces a vortex to intersect the lines $y = \pm 1$:

$$a + r_0 \leqslant 1, \quad \delta \geqslant 2. \tag{22}$$

The equals sign in (22) will lead to the most unstable modes. The equations for λ or A, ϕ_0 are obtained according to (15) and (17), respectively:

$$\left.\begin{aligned}
\beta_{11}\dot{\lambda}+\beta_{12}\dot{A}+\beta_{13}A\dot{\phi}_0 &= \alpha_{11}A^2+\frac{\alpha_{12}}{Re}\lambda+\frac{\alpha_{13}}{Re}A;\\
\beta_{21}\dot{\lambda}+\beta_{22}\dot{A}+\beta_{23}A\dot{\phi}_0 &= \left(\alpha_{21}+\frac{\alpha_{22}}{ARe}\right)\lambda+\frac{\alpha_{20}}{Re}A;\\
\beta_{31}\dot{\lambda}+\beta_{32}\dot{A}+\beta_{33}A\dot{\phi}_0 &= A\,(\alpha_{31}\lambda+\alpha_{32}A+\alpha_{33}).
\end{aligned}\right\} \tag{23}$$

$\alpha_{\nu\mu}$ and $\beta_{\nu\mu}$ are functions of ϕ_0, defined by

$$\left.\begin{aligned}
&\alpha_{11} = -\int_{-1}^{1}\int_{-1}^{1} dx\,dy f_y\psi_{2x}\psi_{2y}; \quad \alpha_{12} = \frac{\delta}{2}\int_{-1}^{1}\int_{-1}^{1} dx\,dy f f_{yy};\\
&\alpha_{13} = -\int_{-1}^{1}\int_{-1}^{1} dx\,dy f_{yyy}\psi_2; \quad \alpha_{21} = -\int_{-1}^{1} dx\,dy f_{yyy}\psi_{2x}\psi_{2y};\\
&\alpha_{20} = \int_{-1}^{1}\int_{-1}^{1} dx fy\,\Delta\psi_2.\Delta\Delta\psi_2; \quad \alpha_{22} = \int_{-1}^{1}\int_{-1}^{1} dx\,dy\,\psi_{2yy}f_{yyy};\\
&\alpha_{31} = \int_{-1}^{1}\int_{-1}^{1} dx\,dy f\,\Delta\psi_{2\phi_0}.\Delta\psi_{2x}-f_{yy}\,\Delta\psi_{2\phi_0}\psi_{2x};\\
&\alpha_{32} = \int_{-1}^{1}\int_{-1}^{1} dx\,dy(\Delta\psi_{2\phi_0x}\psi_{2y}-\psi_{2\phi_0y}\psi_{2x})\,\Delta\psi_2;\\
&\alpha_{33} = -\int_{-1}^{1}\int_{-1}^{1} dx\,dy\,\Delta\psi_{2\phi_0}\Delta\psi_{2x}\,Y \quad \text{for the plane Couette flow};\\
&\alpha_{33} = -\int_{-1}^{1}\int_{-1}^{1} dx\,dy\,\Delta\psi_{2\phi_0}\Delta\psi_{2x}\,(y^2-1) \quad \text{for the Poiseuille flow};\\
&\beta_{11} = \frac{\delta}{2}\int_{-1}^{1}\int_{-1}^{1} dx\,dy f f; \quad \beta_{12} = \int_{-1}^{1}\int_{-1}^{1} dx\,dy f\psi_{2y};\\
&\beta_{13} = \int_{-1}^{1}\int_{-1}^{1} dx\,dy f\psi_{2y\phi_0} = 0; \quad \beta_{21} = \int_{-1}^{1}\int_{-1}^{1} dx\,dy f_y\Delta\psi_2;\\
&\beta_{22} = \int_{-1}^{1}\int_{-1}^{1} dx\,dy\,\Delta\psi_2\Delta\psi_2; \quad \beta_{23} = \beta_{32} = \int_{-1}^{1}\int_{-1}^{1} dx\,dy\,\Delta\psi_2\Delta\psi_{2\phi_0} = 0;\\
&\beta_{31} = \int_{-1}^{1}\int_{-1}^{1} dx\,dy f_y\Delta\psi_{2\phi_0} = 0; \quad \beta_{33} = \int_{-1}^{1}\int_{-1}^{1} dx\,dy\,\Delta\psi_{2\phi_0}\Delta\psi_{2\phi_0}.
\end{aligned}\right\} \tag{24}$$

For sufficiently small Reynolds numbers, equations (23) have only one stationary solution $A = \lambda = 0$, which corresponds to the undisturbed motion. An estimate of the critical Reynolds number is given by the smallest Reynolds number for which equations (23) have a second stationary solution with $A, \lambda \neq 0$.

Similarly to Zahn *et al.* (1974), we compute the stationary solutions of the model. These solutions separate the amplifying states from those which are damped. We consider no solutions which imply profiles of the parallel flow with an overshoot. For physical reasons we require the disturbed velocity profile to be monotonic, which implies the condition

$$\lambda \leqslant \lambda_{\max},$$

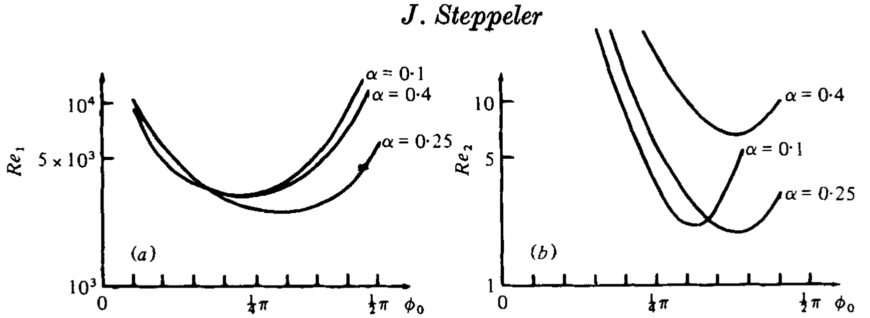

FIGURE 2. Plane Couette flow, $Re_1(a)$ and $Re_2(b)$, as a function of ϕ_0 for different values of the parameter α and $a = 0{\cdot}5$, $\eta = 1$.

with $\lambda_{\max} = 1/|f_y(0)|$ for the plane Couette flow and $\lambda_{\max} = 2\alpha(1-\alpha)$ for the Poiseuille flow. With $\lambda \leqslant \lambda_{\max}$ the last equation of (22) gives an upper bound for A to achieve stationarity:

$$|A| \leqslant \sup_{\lambda \in [0, \lambda_{\max}]} \left| \frac{\alpha_{33} + \alpha_{31}\lambda}{\alpha_{32}} \right|,$$

$$\lambda \in [0, \lambda_{\max}].$$

Since $\alpha_{31\,\max}$ is smaller than 10 % of α_{33}, this term will be neglected in the following estimate. Let $A_s(\phi_0)$ be the value of A which implies $\dot{\phi}_0 = 0$. Neglecting $\alpha_{31}\lambda$ we have

$$A_s(\phi_0) = \frac{\alpha_{33}}{\alpha_{32}}. \tag{25}$$

Now we ask if we can achieve stationary states with $\lambda = \lambda_{\max}$ and $A = A_s$. From the first and second equations of (22) we obtain as a condition of stationarity

$$\left.\begin{aligned} Re &\geqslant Re_1 \\ \text{and} \qquad Re &\geqslant Re_2, \end{aligned}\right\} \tag{26}$$

with
$$Re_1 = -\frac{\alpha_{12}\lambda_{\max} + \alpha_{13}A_s}{\alpha_{11}A_s^2}$$

and
$$Re_2 = -\frac{\alpha_{20} + \alpha_{22}\lambda_{\max}/A_s}{\alpha_{21}\lambda_{\max}}.$$

4. Numerical evaluation of the models

Let us first consider the case that the outer vortex blobs and the centre one have equal radius, $\eta = 1$. Re_1 and Re_2 were computed numerically as functions of the angle ϕ_0. The result for the plane Couette flow with $\alpha = R_0 = 0{\cdot}5$, $\eta = 1$ is shown in figure 2 for different values of the parameter α. One can see that Re_1 defines the more critical condition than Re_2. This was so in all investigated cases. Therefore in the following only Re_1 will be displayed. Figure 3 (a) shows the minimum of the curves in figure 2 and figure 3(b) gives the position of this minimum as a function of α. The minimum Reynolds number for which secondary motion can occur is slightly above 2500 and is obtained for $\alpha = 0{\cdot}27$. To show the dependence of Re_1 on the radius a of the vortex blobs, figure 4 shows for $\alpha = 0{\cdot}27$, $\eta = 1$ the dependence of Re_1 on a. Figure 5 shows the dependence of $\tilde{R}e_{1\,\min}$, defined as the minimum of Re_1 over α and ϕ_0, on a. The

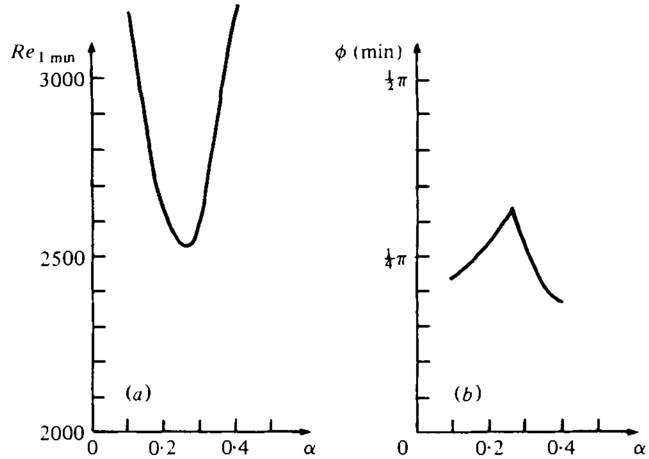

FIGURE 3. Plane Couette flow. (*a*) The minimum of the curves in figure 2 as a function of α; (*b*), the position of this minimum.

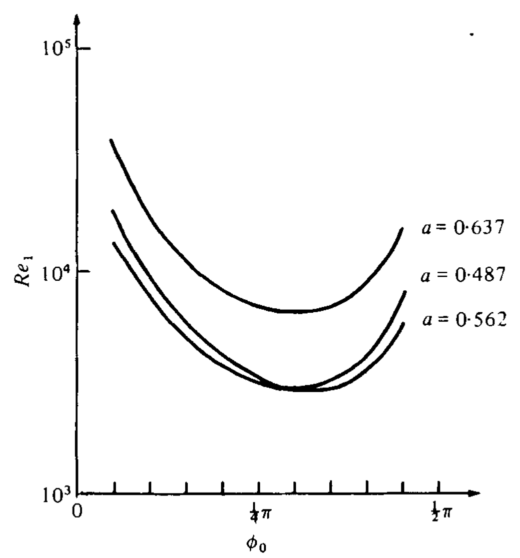

FIGURE 4. Plane Couette flow, Re_1, as a function of ϕ_0 for different values of the radius a for $\eta = 1$, $\alpha = 0{\cdot}27$.

minimum Reynolds number for which instability is possible is 2500 and the instability occurs for a radius a of the vortex blobs slightly above 0·5.

For comparison, we give also the results concerning the Poiseuille flow. Figure 6 is an analogue to figure 2(*a*) and gives Re_1 as functions of ϕ_0 for $\eta = 1$, $\alpha = 0{\cdot}5$ and different values of α. $Re_{1\,\min}$, the minimum of the curves in figure 6, is given as a function of α in figure 7. Figure 8 is an analogue to figure 5 and shows $\tilde{R}e_{1\,\min}$, the minimum of Re_1 over α and ϕ_0, as a function of a. The curves are qualitatively quite similar to those corresponding to the plane Couette flow. However, the Poiseuille flow remains stable for greater Reynolds numbers than the plane Couette flow.

With Fourier modes in the downstream direction, as used by Zahn *et al.* (1974), one needs many modes in order to approximate the vortex blobs used here. For the

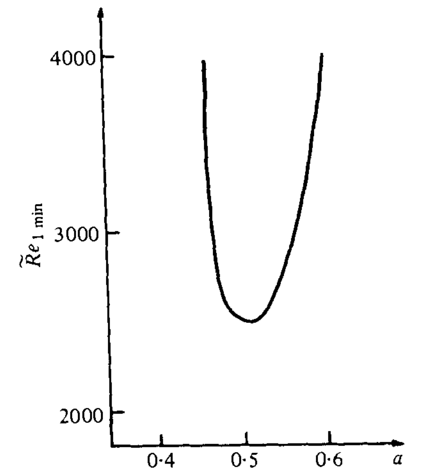

FIGURE 5. $\tilde{R}e_{1\,\mathrm{min}}$, the minimum of Re_1 over α and ϕ_0 as a function of a for $\eta = 1$.

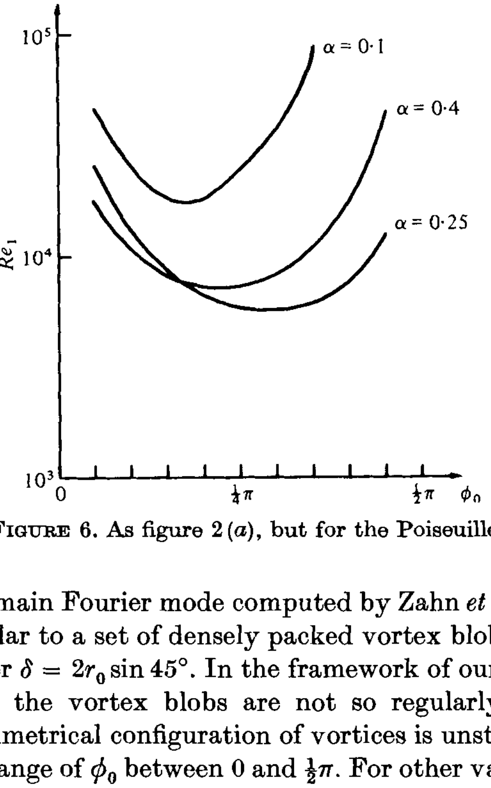

FIGURE 6. As figure 2(a), but for the Poiseuille flow.

Poiseuille flow, the main Fourier mode computed by Zahn *et al.* (1974) corresponds to a flow which is similar to a set of densely packed vortex blobs with $\phi_0 = 45°$ and the repetition parameter $\delta = 2r_0 \sin 45°$. In the framework of our vortex blob mechanics, it is essential that the vortex blobs are not so regularly packed, which means $\delta \geqslant 2(a+r_0)$. A symmetrical configuration of vortices is unstable, because stability is possible only for a range of ϕ_0 between 0 and $\frac{1}{2}\pi$. For other values of ϕ_0 both the shear and the rotation of the blobs around each other would force the vortices into another relative position, while for the indicated range of ϕ_0 these effects compensate each other.

Theories with Fourier modes in the downstream direction need at least two modes to produce an unsymmetric vortex configuration. The main mode computed by Zahn *et al.* (1974) had centre vortices with double the diameter of the two outer ones. This

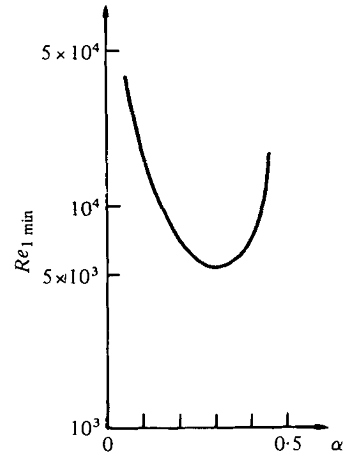

FIGURE 7. As figure 3(*a*), but for the Poiseuille flow.

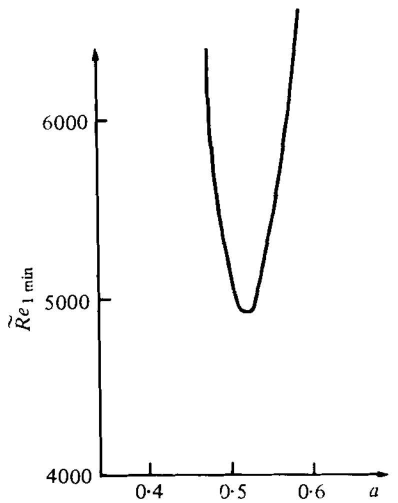

FIGURE 8. As figure 5, but for the Poiseuille flow.

indicates that with our model we may get more unstable modes, when using the centre vortex blob with a greater diameter than the two outer ones. The parameter η in (18) is the relation of the diameter of the outer vortices to that of the centre one.

Figure 9 shows Re_1 as a function of ϕ_0 for the plane Couette flow for different values of η. The values of $a = 0{\cdot}51$ and $\alpha = 0{\cdot}27$ are those which for equal radii had produced the most unstable modes. The corresponding diagram for the Poiseuille flow is shown in figure 10. The most unstable modes are obtained for $\eta = 0{\cdot}5$, corresponding to a centre vortex blob with a diameter equal to the width of the channel.

The critical Reynolds numbers estimated from figures 9 and 10 are 800 for the plane Couette flow and 2000 for Poiseuille flow. Considering the relatively coarse model assumptions, the latter value is in reasonable agreement with the value 2700, obtained by Zahn *et al.* (1974).

The estimate of the critical Reynolds number was based on the assumption that the most unstable modes for $\eta = 0{\cdot}5$ are obtained with the same value of α as for $\eta = 1$.

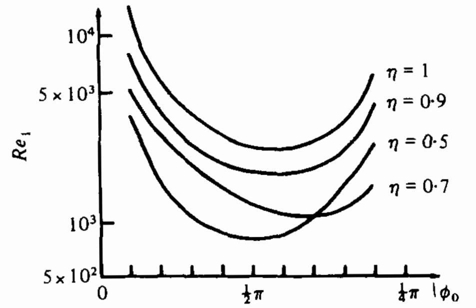

FIGURE 9. Plane Couette flow, Re_1, as a function of ϕ_0 for different values of η and $a = 0{\cdot}51$, $\alpha = 0{\cdot}27$.

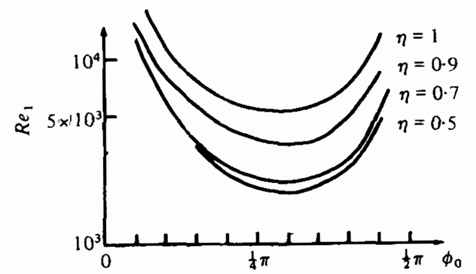

FIGURE 10. As figure 9, but for Poiseuille flow.

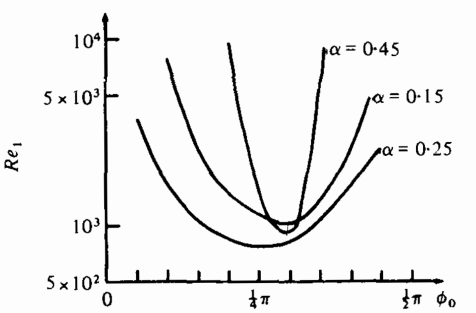

FIGURE 11. Couette flow, Re_1, as a function of ϕ_0 for different values of α for $\eta = 0{\cdot}5$, $a = 0{\cdot}51$.

To check this assumption, figure 11 shows Re_1 as a function of ϕ_0 for different values of α with $\eta = 0{\cdot}5$, $a = 0{\cdot}51$ for the plane Poiseuille flow. The corresponding diagram for the plane Couette flow is shown in figure 12. The figures indicate that indeed for values of about $0{\cdot}27$ the most unstable modes occur.

5. Conclusions

In spite of the simplicity of the model investigated, quasistationary states of the secondary motion were obtained. This was possible because of the nonlinear dependence of the test functions on the parameter ϕ_0, determining the relative position of the three vortex blobs.

The computed critical Reynolds number was for the Poiseuille flow in reasonable

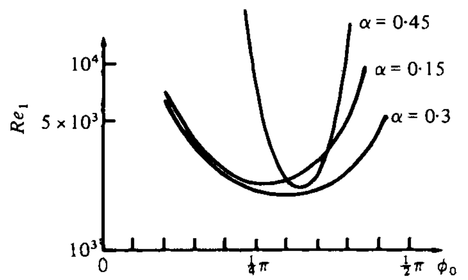

FIGURE 12. As figure 11, but for plane Poiseuille flow.

agreement with that of other computations. For the plane Couette flow the computed critical Reynolds number was 800.

The computation was based on describing a system of vortex blobs by a small number of parameters. A parameter determining the position of a vortex blob was introduced as a dynamical variable. Because this method needs comparatively small computer capacity, it may be useful in more complicated situations, for example the computation of the decay of a large vortex blob into smaller ones.

The comments on the manuscript of several members of the Max Planck Institut für Strömungslehre were appreciated.

REFERENCES

COFFEE, T. 1977 *J. Fluid Mech.* **83**, 401.
DAVEY, A. 1973 *J. Fluid Mech.* **57**, 369.
EASON, E. D. 1976 *Int. J. Numerical Methods in Engng* **10**, 1021.
FINLAYSON, B. A. 1972 *The Method of Weighted Residuals and Variational Principles.* Academic Press.
GALLAGHER, A. P. & MERCER, A. McD. 1964 *J. Fluid Mech.* **13**, 91.
GROHNE, D. 1954 *Z. Angew. Math. Mech.* **34**, 344.
HERBERT, TH. 1976 *Proc. 5th Int. Conf. Num. Meth. Fluid Dyn.*, p. 235. Springer.
LORFNZ, E. N. 1963 *J. Atm. Sci.* **20**, 130.
OGURA, Y. & YAGIHASHI, A. 1969 *J. Meteor. Soc. Japan* **47**, 437.
ORSZAG, S. A. 1971 *J. Fluid Mech.* **50**, 689.
PEKERIS, C. L. & SHKOLLER, B. 1969*a* *J. Fluid Mech.* **39**, 611.
PEKERIS, C. L. & SHKOLLER, B. 1969*b* *J. Fluid Mech.* **39**, 629.
PEKERIS, C. L. & SHKOLLER, B. 1971 *Proc. Nat. Acad. Sci.* **68**, 197.
REYNOLDS, W. C. & POTTER, M. C. 1967 *J. Fluid Mech.* **27**, 465.
STEPPELER, J. 1978 *Int. J. Computers and Fluids* **6**, 2S1.
STUART, J. T. 1958 *J. Fluid Mech.* **4**, 1.
STUART, J. T. 1960 *J. Fluid Mech.* **9**, 353.
VICHENEVETSKY, R. 1969 *IEEE Transactions on Computers*, C **18**, 499.
WATSON, J. 1960 *J. Fluid Mech.* **9**, 371.
ZAHN, J. P., TOOMRE, J., SPIEGEL, E. A. & GOUGH, D. O. 1974 *J. Fluid Mech.* **64**, 319.